4th IAA Planetary Defense Conference – PDC 2015
13-17 April 2015, Frascati, Roma, Italy

IAA-PDC-15-02-10

ASTEROIDS COUPLED DYNAMICS ANALYSIS BY MEANS OF ACCURATE MASS DISTRIBUTION AND PERTURBATIONS MODELING

Andrea Colagrossi(1), Fabio Ferrari(2) and Michèle Lavagna(3)

(1) *Politecnico di Milano, Via La Masa 34, 20156, Milano, Italy, andrea.colagrossi@mail.polimi.it*

(2) *Politecnico di Milano, Via La Masa 34, 20156, Milano, Italy, +390223998365, fabio1.ferrari@polimi.it*

(3) *Politecnico di Milano, Via La Masa 34, 20156, Milano, Italy, +390223998364, michelle.lavagna@polimi.it*

Keywords: *Asteroid, Gravity Field, Mass Distribution, Disturbances, Rotation.*

ABSTRACT

One of the most important aspects when dealing with a Potentially Hazardous Object (PHO) is the accurate determination of its dynamical state. In particular, the determination of orbital and rotational perturbations is important to propagate accurately the heliocentric orbital path of an asteroid or a comet, and to be more precise in the impact risk determination and related uncertainty containment. The paper discusses the analysis and study of the motion of an irregularly-shaped celestial body, with particular attention to its complex three-dimensional rotational dynamics: the rotation state, nutation and precession motions are considered while modelling. All perturbations, relevant to the case of study, are included in the dynamical model, from the classical to the more complex, such as the Solar Radiation Pressure (SRP), the third body gravitational effect (presence of the Sun), the YORP effect and the internal dissipation of energy. In addition, particular attention has been paid to accurately model the shape of the asteroid: simple spherical models demonstrated to possess low accuracy when the asteroid or the comet is not spherically shaped. Irregular shapes represent, indeed, one of the most important aspects to compute the disturbances affecting the dynamics of these objects. The study has been performed by considering different characteristic shapes for typical irregular bodies: from the quasi-spherical, to the dog-bone and the elongated shapes. The perturbations due to external sources are modelled numerically. The sources of disturbances are then ranked and different criteria to propagate rotational motion have been derived depending on the shape of the observed asteroid. Even if the simulation results have been verified on selected asteroids dynamics, the presented methods and approach apply to the dynamical propagation of any kind of asteroid or comet.

INTRODUCTION

Celestial bodies with irregular shapes are exposed to increasing interest in the scientific community. They are extremely numerous in the Solar System, and even if they comprise a tiny fraction of the mass orbiting around the Sun, their study is fundamental to understand the formation and the evolution of the Solar System, as well as the origin of the more massive celestial objects. In fact, *asteroids* and *comets* represent fragments and tiny pieces left over from the process that formed the inner plan-

ets, including Earth. Moreover, carbon-based molecules and volatile materials, which were fundamental to establish life, may have been carried to Earth during the early life of the Solar System, through the impacts of these minor celestial bodies.

In addition, some of these small Solar System's bodies are catalogued as *potentially hazardous objects* (PHO), meaning that their orbit could make close approaches to the Earth and they are massive enough to provoke a serious devastation in the event of impact. Consequently, they have to be carefully analysed to understand their composition, structure, size and future trajectories, in order to be able to devise an intelligent strategy to protect the Earth from the risk of an eventual cosmic collision.

The rotational state of an irregular celestial body is important to propagate accurately its heliocentric orbital path, and to be more precise in the impact risk determination. Since, in this way, the interactions of the body with the external environment can be precisely evaluated. Furthermore, the understanding of the spin-vector evolution of small celestial bodies could be applied to study the formation and the chaotic events that created the Solar System. For instance, according to (Lupishko, 2014) the rotation rates distribution of near-Earth asteroids is noticeably different from the analogous distribution of Main Belt asteroids, in consequence of an excess of fast and slow rotators, which are not so conspicuous in the distribution for the bodies in the Main Belt.

All these investigations can be performed with a model that is able to describe and simulate the rotational dynamics of an asteroid. In this paper, the model is implemented starting from the equations of rotational dynamics and including all the relevant perturbing effects, such as the Solar Radiation Pressure (SRP), the third body gravitational influence, the YORP effect and the internal dissipation of energy. Their contribution is numerically computed, exploiting a polyhedron shape discretization. In this way, the only approximation that is made is the one of discretizing the actual shape of the body with a polyhedron, and the obtained value is a good estimation of the real one. Moreover, the shadows and the self-shadowing phenomenon can be considered with a simple analysis of the geometry of the problem.

The algorithm is accurately validated and the results are shown. In fact, some of them are particularly interesting to delineate the effect of the analysed perturbations on the dynamical evolution of Solar System's irregular objects. In addition, some simulations are presented and discussed, and a sensitivity analysis to evaluate the robustness of the entire research is considered.

BACKGROUND AND MODEL DEFINITION

SHAPE MODEL

The presented dynamical model deals with an irregularly-shaped rigid body, which is modelled by means of a polyhedral shape discretization. This is obtained performing a *Delaunay triangulation* in a 3D Euclidean space, staring from topographical data expressed in a vertex list, which is usually obtained from ground observations or radio tracking data coming from a space mission. In figure 1, the shape model for the asteroid 433 Eros is shown as example, with data coming from (Miller, 2002).

The irregular object is assumed to have an unperturbed orbital motion, evolving in a

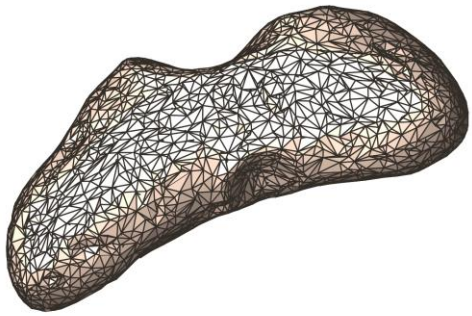

Figure 1: Polyhedron Shape Model for 433 Eros. (Shape Data Credits: NASA, Johns Hopkins APL, NEAR, Multi-Spectral Imager, 2002 Miller et al.)

circular and planar orbit around the Sun with radius equal to the semi-major axis of the real orbit of the body. This simplifying assumption is made in order to focus the attention only on the rotational dynamics. Moreover, the model is developed in a rotating frame that is fixed with respect to the irregular body and it is aligned with the principal inertia axes of the shape model. In this work, the total mass of the objects is taken from the literature and then the rotational inertia properties of the body are computed exploiting the information coming from the shape model.

The bodies that will be analysed in this paper are: 67P Churyumov- Gerasimenko (67P C-G) comet, 216 Kleopatra Main-Belt asteroid, 4179 Toutatis Apollo-Alinda asteroid, 433 Eros Amor asteroid and 1580 Betulia Amor asteroid. These data are all coming from the Rosetta Mission of ESA, from the Planetary Data System Asteroid and Dust Archive of NASA and from the Asteroid Radar Research Group of JPL. In table 1, the corresponding mass values are reported, while in table 2, the obtained moments of inertia are listed.

EQUATIONS OF MOTION

The equations of motion describing the rotational dynamics of the irregular body are the Euler's equations of rigid body motions, which can be expressed in principal inertia reference as:

$$\mathbf{I}\dot{\boldsymbol{\omega}} + \boldsymbol{\omega} \times \mathbf{I}\boldsymbol{\omega} = \mathbf{m}, \tag{1}$$

where $\boldsymbol{\omega}$ is the angular velocity in the body-fixed reference, $\mathbf{I}$ is the principal inertia tensor and $\mathbf{m}$ is the external torque in the same coordinate system. This is a vectorial quasi-linear first-order ordinary differential equation that can be integrated numerically, and for this purpose, a system of three scalar first order differential equations is preferred. The equation (1) is solved together with the equations of rotational kinematics to have the evolution of the rotation state in time, by means of the direction cosine matrix, $\mathbf{A}$. The perturbing torques are evaluated in the rotating frame at each

Table 2: Mass of selected irregular bodies.

		M [kg]
67P	C-G	1.00×10^{13}
216	Kleopatra	4.64×10^{18}
4179	Toutatis	5.00×10^{13}
433	Eros	6.69×10^{15}
1580	Betulia	1.63×10^{14}

Table 2: Principal moments of inertia of selected irregular bodies.

		I_x [kg m^2]	I_y [kg m^2]	I_z [kg m^2]
67P	C-G	9.64×10^{18}	1.74×10^{19}	1.86×10^{19}
216	Kleopatra	3.05×10^{27}	2.08×10^{28}	2.10×10^{28}
4179	Toutatis	1.86×10^{19}	5.58×10^{19}	5.92×10^{19}
433	Eros	1.02×10^{23}	4.93×10^{23}	5.01×10^{23}
1580	Betulia	4.21×10^{20}	5.02×10^{20}	6.36×10^{20}

integration step; they are then combined together and inserted in equation (1).

THIRD BODY GRAVITATIONAL EFFECT

The gravitational effect of the Sun is accounted with the usual expression of the gravity gradient, since the gravitational attraction of the third body is not uniform, and the non-symmetric body experiences a disturbing torque. If one principal inertia axis is aligned with the Sun-Body direction, the torque is null. Moreover, this torque depends on the relative orientation of the body with respect to the Sun and thus, if averaged over one full rotation of the asteroid or comet on its axis, and over one full revolution as it orbits the Sun, the secular contribution vanishes. The body is assumed infinitely rigid and no tidal deformation is taken into account. Therefore, the shape of the asteroid or the comet is preserved and the tidal torque is not considered.

SOLAR RADIATION PRESSURE

The force that is generated by the solar radiation pressure interaction can be computed for each triangular face of the polyhedron model, and then the global force can be found summing all over the single contributions. In this way, it is possible to use the expression for the radiation pressure on a flat surface. The incident radiation coming from the Sun can be absorbed, specularly reflected and reflected with diffusion. The fraction of radiation associated with each one of these interaction modes is expressed by a coefficient of absorption, $c_a = 0.9$, diffuse reflection, $c_d = 0.075$, and specular reflection, $c_s = 0.025$. Obviously, these coefficients sum to unity.

The self-shadowing phenomenon can be considered with a simple analysis of the geometry of the problem. For this particular purpose, the Sun is considered at an infinite distance from the body and dimensionless. Consequently, the shadow, being generated by a point source, is composed only by the *umbra*. The shadowing algo-

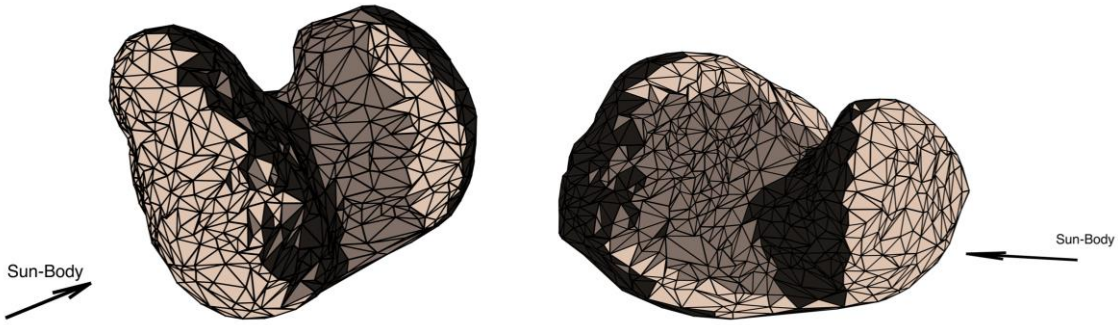

Figure 2: Shadowing algorithm output. (The illuminated faces are pale brown, the self-shadow faces are dark brown and the shadow faces are almost black. The Sun-Body direction is indicated in the figure.)

rithm begins detecting all the triangular faces that are not directly facing the Sun: the *shadow faces*. They are recognized if the projection of their outward normal vector on the Sun-Body direction is positive. Then, among the remaining faces, the *self-shadow* ones are detected if the semi-infinite vector from the centre of the face, parallel to the Body-Sun direction in the rotating frame, intersects the shape model. This is made possible with a query on the Delaunay triangulation, which is able to find the intersections between a vector and the polyhedron mesh. Only the remaining *illuminated faces* are then used to compute the torques due to solar radiation. This algorithm is executed at each integration step and it makes use of parallel computing techniques, improving the computational speed of the whole algorithm. An example of the shadowing algorithm output is shown in figure 2.

YORP EFFECT

The Yarkovsky–O'Keefe–Radzievskii–Paddack (YORP) effect is the other disturbing contribution related with the interaction of the radiation with the surface of the body. In this case, it takes into account the emission of thermal photons related with the diurnal heating of a rotating space object. This effect can produce torques that affect the spin rate and spin axis orientation of small irregular celestial bodies. The torque acting on an object is small, since the amount of momentum carried by photons is limited. Nevertheless, the YORP torque is secular, so that after a long period the body's rotation state can be noticeably different. There are several analogies with the solar radiation pressure, and they are separately addressed only because the YORP effect deals with the radiation emitted by the body, while the solar radiation pressure deals with the incoming radiation from the Sun, which is absorbed or reflected. Obviously, the thermal balance of the body couples these contributions, and therefore, their differences are more formal than conceptual. Its contribution can be computed as in (Rubincam, 2000), with:

$$\mathbf{m}_{YORP} = \frac{2}{3}(1-\alpha)P_S \sum_{i=1}^{N} A_i(\,\hat{\mathbf{n}}_i \times \boldsymbol{\rho}_i)\cos(\theta_i), \tag{3}$$

where α is the albedo of the body, P_S is the pressure due to the Sun radiation, A_i is the area of each face and $\hat{\mathbf{n}}_i$ the unit vector normal to the surface. Moreover, $\boldsymbol{\rho}_i$ is the position of each triangular face's centre with respect to the centre of mass of the

body and θ_i is the angle between the Body-Sun and the normal to the surface directions. Therefore, even in this case, the force is computed for each singular planar face, considering shadows and self-shadowing; then, the global contribution is obtained thanks to a summation all over the polyhedron shape. In this model, it is assumed that the body surface is Lambertian, i.e. the reaction force from photons departing from any given surface elements is normal to it.

The differential YORP force acts on the normal to the surface direction, as the specularly reflected solar radiation pressure. This characteristic determines the secularity of the YORP torque. On the contrary, the radiation forces along the Body-Sun direction, e.g. absorbed SRP, average to zero, because they depend on the projection that the body presents to the Sun: these solar torques cancel over one full rotation and one full revolution as the Sun sees the projection in all directions.

INTERNAL ENERGY LOSSES

Energy losses in an inelastic material occur when the internal stresses are time-variant; hence, even freely rotating bodies in space lose energy because internal stresses are associated with the accelerations caused by nutation. Therefore, internal dissipation of energy is associated with non-principal rotation states, since in this case the rotational acceleration is time-varying in the body-fixed frame. In presence of internal energy losses, the angular momentum vector of the body tends to align with its maximum inertia axis, and even though this effect is extremely small, it can influence the rotational state of a small wobbling celestial object, if a long time scale is taken into account. This effect can be modelled with an additional perturbing torque in the equations of motion, according to (Cicalò, 2010). It is influenced by the shape of the body, its density, the rigidity of the material and the inclination of the spinning axis with respect to the principal inertia directions. However, the dissipation of energy is mainly affected from the angular momentum magnitude, present with its cube value in the equation to compute this contribution. In general, the energy loss phenomena is less important than the other perturbative effects and thus, the non-principal axis state can be an asymptotic state, even if this contribution is taken into account. On the contrary, with a large angular momentum, the dissipation of energy could dominate the other perturbing torques.

The results of the model can be analysed by means of several quantities and, in this work angular momentum, kinetic energy, obliquity and dynamic inertia are employed. The obliquity, δ, describes the direction of the angular momentum vector in the inertial reference: it is the angle between the normal to the orbital plane and the angular momentum vector. The dynamic inertia can be related with the non-principal rotation mode of the body, and it is computed as:

$$I_D = \frac{h^2}{2T}, \tag{3}$$

where h is the magnitude of the angular momentum and T is the kinetic energy of the rotating body. If the body is in principal axis rotation state, the dynamic inertia is equal to the related principal moment of inertia.

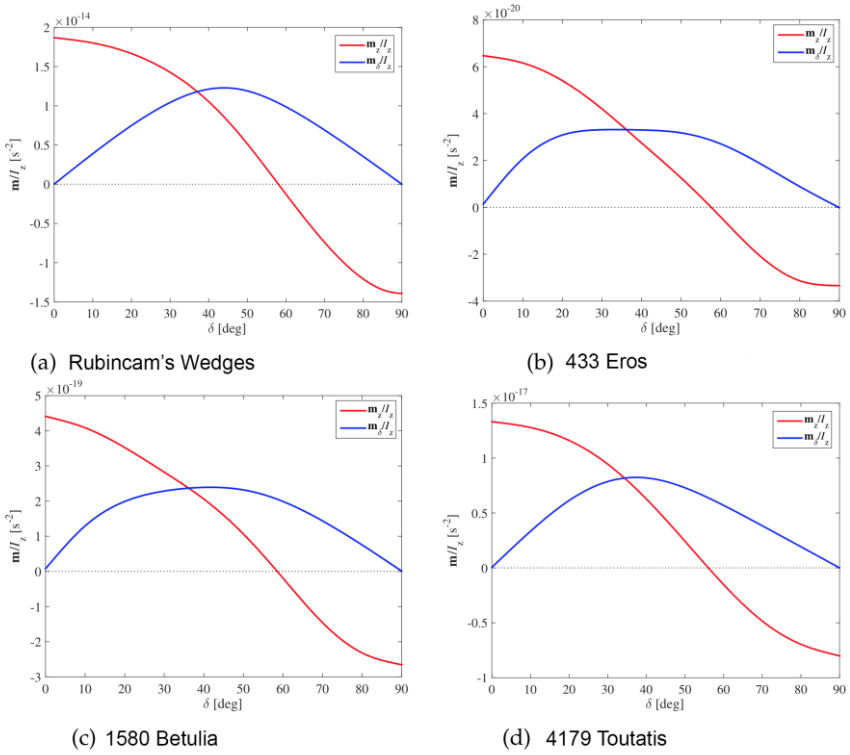

Figure 3: Validation of YORP.

MODEL VALIDATION

The model is validated thoroughly with different simulations, and all the perturbing torques are individually computed and verified. Some results are well known, but the results obtained on the torques due to the solar radiation are quite interesting and give an interesting overview of the whole phenomenon. Indeed, the solar radiation pressure and the YORP effect are validated together, since their effect can be compared. The YORP effect and the reflected solar radiation pressure acts normally to the surface direction, while the absorbed radiation generates a force in the Sun-Body direction. The validation procedure was performed exploiting the averaged quantities over one full rotation and over one full revolution of the body. The results are shown in figure 3 for the YORP effect and in figure 4 for the solar radiation pressure. They are obtained evaluating the perturbing torque for every 10˚ of rotation and revolution; these values are then averaged and saved for different values of obliquity. Two particular components of the torque $\mathbf{m}_z$ and $\mathbf{m}_\delta$ are used to display the outcomes. $\mathbf{m}_z$ is the torque along the spin axis which changes the rotation rate, while $\mathbf{m}_\delta$ acts to change the obliquity. The torques are normalized with respect to the maximum moment of inertia.

The behaviour of the YORP effect is very similar for all the asteroids; it is almost independently from the shape of the body. Moreover, all the bodies are influenced by this perturbing torque similarly to the *Rubincam's wedges*. This simple but insightful shape was introduced by David Rubincam, in (Rubincam, 2000), to explain the radiative torques on irregular celestial bodies. This object has the “windmill” asymmetry that is needed in order to see the effect of the YORP torque; axisymmetric figures are not influenced by this perturbation on a long period.

The component in the direction of the normal to the surface of the solar radiation

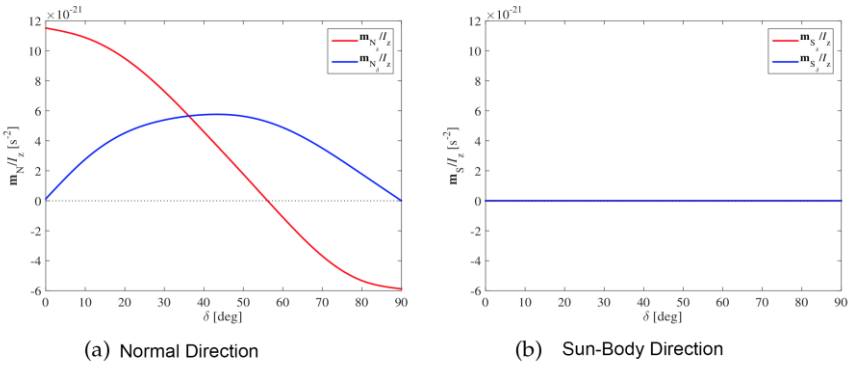

Figure 4: Validation of SRP.

pressure obviously behaves like the YORP effect, but the component along the Sun-Body radius vector averages to zero, as expected.

The Rubincam's wedges are the most influenced by the thermal torques, because of their shape to enhance the contribution of these perturbations. The value of the perturbing accelerations indicates the amount “radiative-windmill” asymmetry of each shape. Then, it can be noted that the secular contribution of the YORP is larger than the one of the solar pressure. The reason is that the majority of the incident solar radiation is absorbed by the celestial bodies, since they are usually dark. However, the absorbed radiation has effect along the Sun-Body direction; thus, it perturbs the body only with a non-secular contribution. The emitted thermal photons are connected with the incident absorbed energy, and as a consequence, the low albedo of the actual celestial bodies determine the prevalence of the YORP effect over the solar radiation pressure for long time scales.

For what concern, the dissipation of energy influences only non-principal rotation states, which have been simulated to validate this contribution. The motion in presence of this effect tends to the condition of minimum energy, with the body rotating around the maximum inertia axis. When the pure spin state is reached the dissipation of energy does not influence the motion anymore and the dynamics is stable.

SENSITIVITY ANALYSIS

A sensitivity analysis has been carried out, in such a way that the uncertainties in the input data are correlated to the uncertainties in the outpu, and the robustness of the model can be rationally estimated. The study that is here presented is applied to uncertainties in the mass, in the shape model and in the rotational state determination of the selected celestial body.
Realistic values for typical uncertainty intervals are present in the literature, even though a unique characterization does not exist. For example, in (Hilton, 2002) the inertia properties are usually determined within 5% and 40% of accuracy; here the mass is assumed to have a tolerance of ±30%. For what concern the shape model, the typical error is about 10-50%, according to (Nolan, 2013); in the current analysis, the polyhedron model is reshaped between an extremely Lo-Fi model, ~250 faces, and a Hi-Fi model, ~5000 faces, with a resulting uncertainty on the shape related quantities of ±15%. Finally, considering the rotational state, the rotation period is commonly determined with a good accuracy, while the orientation of the spin axis has often a tolerance of some degrees (Barucci, 1986). Hence, in this sensitivity

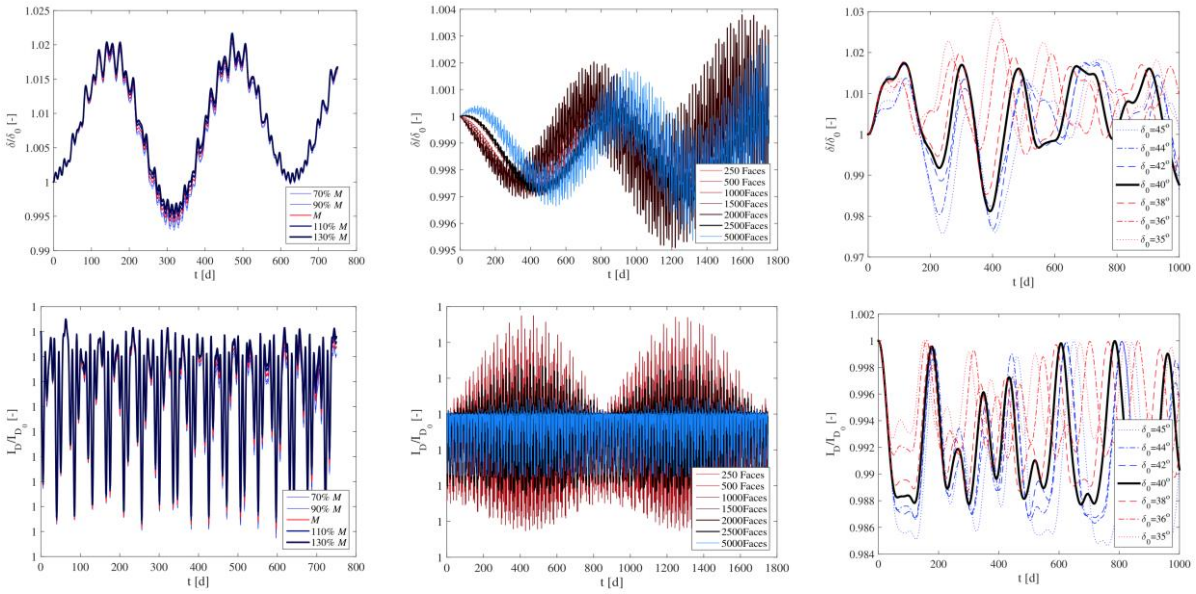

(a) Mass Sensitivity (b) Shape Sensitivity (c) Rotation Sensitivity

Figure 5: Results of the sensitivity analysis.

analysis, the magnitude of the angular velocity is maintained constant and the initial spin axis direction is allowed to vary within ±5˚. The results are shown in figure 5.

The sensitivity analysis on the mass of the body is shown in figure 5(a), where the obliquity and the dynamic inertia are normalized with respect to their respective values, δ_0 and I_{D_0}, computed at the generic reference time $t = 0$. The object that is used in this study is the asteroid 433 Eros. The uncertainties in mass determination do not significantly affect the propagation of the perturbed rotational dynamics for an irregular celestial body. In fact, in all the different simulations the motion remain very close to the real one, red line, and the evolution of the represented quantities always follows the same trend. This result makes sense, since the perturbing torques are identical for all the tested mass values, and obviously, only the acceleration levels are different. Accordingly, the behaviour of the heavier asteroids is opposite to the one of the objects with a smaller mass, with the real case bounded between the two opposite scenarios.

The sensitivity analysis for the different shapes is performed for 216 Kleopatra and the results for the relative values of the dynamic quantities are shown in figure 5(b). In this case, the differences between the different analysed resolutions are larger than those in for the mass. Here, the different shapes have different interactions with the perturbations, and thus, the dynamical evolutions follow slightly separate trends. However, this gap is not so wide and the propagation of the rotational motion is robust enough with respect to the errors in the shape determination. Even the extremely Lo-Fi model, red thin curve, stays in the vicinity of the general behaviour, proving that a rough estimation of the perturbative effects can be accomplished with a coarse shape discretization. It is worthwhile to point out that, in this analysis, only the perturbation acting on the surface, e.g. YORP and solar radiation pressure are influenced by the shape model.

Table 3: Magnitude of Perturbing Torques

		$\|\mathbf{m}_{GG}\|$ [N m]	$\|\mathbf{m}_{SRP}\|$ [N m]
67P	C-G	7.87×10^{3}	7.86×10^{2}
216	Kleopatra	3.11×10^{13}	2.30×10^{7}
4179	Toutatis	7.25×10^{4}	3.90×10^{2}
433	Eros	4.68×10^{9}	5.62×10^{5}
1580	Betulia	3.29×10^{5}	3.12×10^{3}

		$\|\mathbf{m}_{YORP}\|$ [N m]	$\|\mathbf{m}_{D}\|$ [N m]
67P	C-G	5.06×10^{2}	3.35×10^{-2}
216	Kleopatra	2.16×10^{7}	7.44×10^{12}
4179	Toutatis	2.48×10^{2}	2.20×10^{-3}
433	Eros	5.58×10^{5}	2.26×10^{6}
1580	Betulia	2.12×10^{3}	8.44×10^{2}

The sensitivity analysis on the rotation state is applied to 4179 Toutatis, whose rotation state is well known, but variable in time. This body is in a complex non-principal rotation state and the angle between the angular velocity vector and the minimum inertia axis varies between 21.16° and 20.90°. This sensitivity can have a dual meaning. In fact, the uncertainty in the direction of the spinning axis can be interpreted as: the possible error in the rotation state determination for a generic asteroid; the possible dynamical evolution of Toutatis if a space probe rendezvouses with it at a certain time, which is different from the scheduled time, and thus, the mission must be correspondingly modified. The reference spinning axis direction has 40° of initial obliquity. Comparing the effects on the propagation of the dynamics, the ones due to the errors on the rotation axis direction are stronger than those related with the inaccuracies on mass and shape determination. Nevertheless, the gap between the different simulations is still limited and the trends of the analysed quantities are remarkably similar. For $t = 0$, one principal axis is aligned with the Sun, i.e. there is no gravity gradient torque, and the dissipation of energy can be neglected. So, taking into account only the radiative perturbations, the examples with a lower obliquity experiences a larger spin torque, $\mathbf{m}_z$, and their dynamics is faster. In general, also in the case of uncertainties in the rotational state determination, the model is robust enough, and the dynamic quantities are bounded in the vicinity of the reference solution, without any chaotic divergence.

MAGNITUDE OF PERTURBING TORQUES

The magnitudes of the different perturbation are listed in table 3 for the reference irregular celestial objects. These values are obtained computing the norm of the root mean squares of the torques components, evaluated along one orbital period. The simulations are performed using the real rotation state of the selected objects as initial conditions.

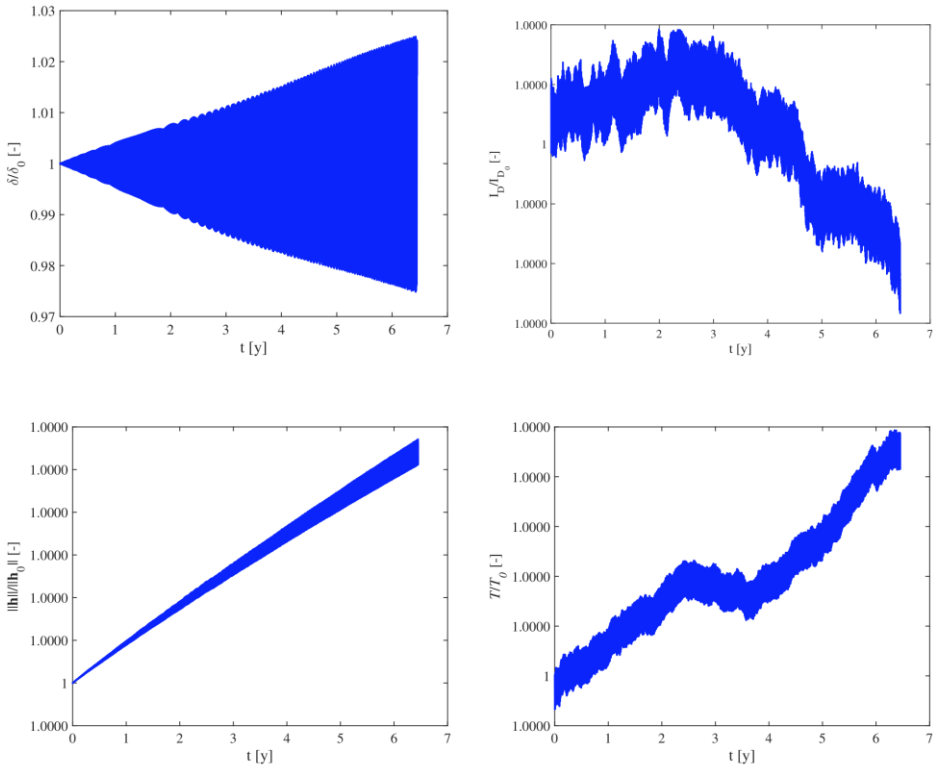

Figure 6: Simulation on 67P Churyumov-Gerasimenko.

The gravity gradient torque is the largest perturbative effect, but as already said, it has not a secular effect. The periodic fluctuations in the dynamics of the body are mainly due to this component. The dissipation of energy is the least influencing term and its contribution is practically negligible in the short period. The big and fast spinning asteroids Kleopatra and Eros are the only exceptions to this last consideration. In fact, the large inertia properties and the rotation state of these two bodies determine a considerable torque due to the internal friction. In addition, the two perturbations due to solar radiation affect mainly the rotation rate of asteroids a few kilometres in diameter (Bottke Jr, 2002). Therefore, Kleopatra and Eros have a frictional torque that is some order of magnitudes larger than the YORP and the solar radiation pressure effects.
The magnitude of the two radiative torques is comparable, since the emitted and the incident radiations are connected by the thermal balance of the body. The emitted energy is a fraction of the whole incident flux, and consequently, the YORP produces a torque that is slightly smaller than the one due to the solar radiation pressure. However, the secular effect is principally related with the YORP effect.

APPLICATION OF THE MODEL

As a last example of the output of the developed model: a simulation on the comet 67P Churyumov-Gerasimenko, is reported in figure 6. The simulated data refer to the present rotation state of the body, as measured in 2014 by the European Space Agency's Rosetta mission and they are different from those acquired during the 2009 perihelion passage. This change in the rotation rate of 67P was probably due to sublimation-induced torques, which are not considered in this work, and thus, the pre-

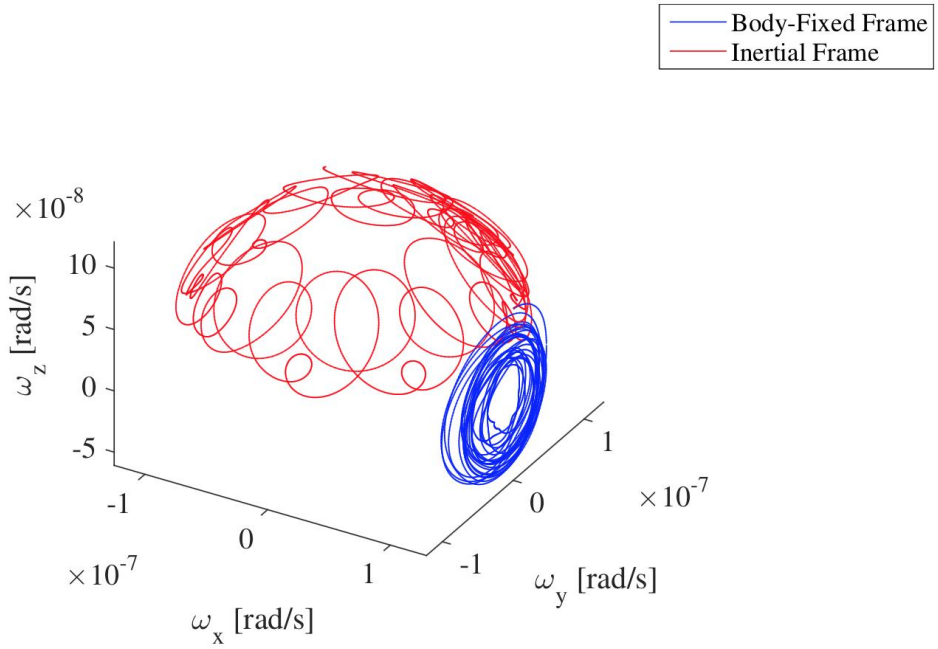

Figure 7: Simulation on 67P Churyumov-Gerasimenko, reduced spinning rate.

sent analysis is valid when the object is far from the Sun and the comet activity is low enough. The assumption to have the orbital motion in a circular orbit with radius equal to 3.46 AU is compatible with this requirement. The dynamics has been simulated for one orbital period of the comet around the Sun.
In this case, the rotation state of the comet 67P is evidently in a stable condition: the secular variation of the considered quantities, in the simulated period, is extremely small. In addition, the periodic oscillations are also limited and the rotation state can be practically considered constant in time. However, in the plots some trends can be clearly detected: the increase in the kinetic energy and angular momentum and the decrease of dynamic inertia. The reduction in the dynamic inertia is representing the spinning axis that is slowly departing from the maximum inertia axis, as can be similarly understood from the increase in the oscillation of the obliquity. This means that the nutation motion is becoming more important, because of the perturbation that progressively tilts the rotation axis. In the meantime, the kinetic energy and the angular momentum increase, and the only compatible solution is determined by the increase in the magnitude of the angular velocity. In order to explain this point, the secular effect of the radiative perturbations should be considered. The YORP and the solar radiation pressure spin-up the small Solar System's bodies for $\delta < 55°$, and so, the angular velocity of 67P correctly has a raising trend. The effect of the dissipation of energy is negligible since the rotational dynamics of the body has a small nutation component and a not sufficiently fast spinning rate.

In addition, in figure 7, the dynamics of 67P Churyumov-Gerasimenko is simulated for 100 years. In this case, the initial conditions for the rotational motion are arbitrarily assumed, with the spinning axis inclined of 30° with respect to $\hat{\mathbf{x}}$ and a rotation period of 1 year. These values are completely unrealistic, but they are employed to highlight the effect of the perturbations, because the rotational dynamics is less stiff, if the body has a slow spinning rate. In this simulation, the motion is particularly affected by the perturbations and the secular variation is evident. In spite of that, there

is not diverging chaotic component of the motion and the trajectory is bounded in a region close to the initial conditions. The perturbative effects do not destabilize the rotational dynamics of the considered object. The same trajectory of the angular velocity, evaluated in the inertial space, is interesting to understand the relation between the two systems of reference. Moreover, precession and nutation motions are particularly clear in this perspective, showing the complex dynamical evolution of a perturbed slow spinning body in non-principal rotation state.

CONCLUSIONS

The rotation motion is markedly affected by the presence of the perturbations. Their effect is different for each single case, but in general, radiative torques and third body gravitation are the most disturbing terms. However, only the radiation that acts in the direction normal to the surface has a relevant secular contribution. Hence, the long-term evolution of the rotational dynamics of an irregular celestial body is mainly influenced by the YORP effect. Yet, since the non-periodic influence of the perturbations is particularly small, the time scale of these secular effects is exceptionally long and they can be neglected for preliminary short-term simulations. Nevertheless, all the perturbing torques determine fluctuations in the rotation state of the analysed object.
The perturbations have been meticulously modelled, exploiting the polyhedron shape; per contra, the precision of the available data is not always guaranteed; therefore, the performed sensitivity analysis ensures the validity of the conclusions regardless of the fidelity to which the properties of the body are determined. The results show that the dynamical model is robust enough, and within the typical range of uncertainty, the simulations are sufficiently correct. The global evolution of the motion is preserved, and it is reasonable to use the accurate dynamical model, even though the physical and dynamical characteristics of the celestial object are just a preliminary estimate.

BIBLIOGRAPHY

Barucci, M. B. *et al.* (1986). Asteroid spin axes-two additional pole determi- nations and theoretical implications . *Astronomy and Astrophysics , 163*, 261-268.
Bottke Jr, W. F. *et al.* (2002). The effect of Yarkovsky thermal forces on the dynamical evolution of asteroids and meteoroids . *Asteroids III , 395*.
Cicalò, S. *et al.* (2010). Averaged rotational dynamics of an asteroid in tumbling rotation under the YORP torque . *Celestial Mechanics and Dynamical Astronomy , 106* (4), 301-337.
Hilton, J. L. (2002). Asteroid masses and densities . *Asteroids III , 1*, 103-112.
Lupishko, D. *et al.* (2014). Influence of the YORP effect on rotation rates of near-Earth asteroids . *Meteoritics and Planetary Science , 49* (1), 80-85.
Miller, J. K. *et al.* (2002). Determination of shape, gravity, and rotational state of asteroid 433 Eros . *Icarus , 155* (1), 3-17.
Nolan, M. C. *et al.* (2013). Shape model and surface properties of the OSIRIS-REx target asteroid (101955) Bennu from radar and light curve observations . *Icarus , 226* (1), 629-640.
Rubincam, D. P. (2000). Radiative spin-up and spin-down of small aster- oids . *Icarus , 148* (1), 2-11.